

AD-A182 262

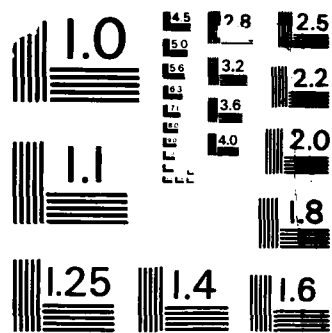
NMR DSC TMA AND HIGH PRESSURE ELECTRICAL CONDUCTIVITY
STUDIES IN PPO COMP (U) HUNTER COLL NEW YORK DEPT OF
PHYSICS AND ASTRONOMY S G GREENBAUM ET AL 01 JUL 87
TR-7 N00014-85-K-0304 F/G 11/10

1/1

UNCLASSIFIED

NL

END
8-87
DTIC



MICROCOPY RESOLUTION TEST CHART
NATIONAL BUREAU OF STANDARDS-1963-A

AD-A182 262

12

OFFICE OF NAVAL RESEARCH
Contract N00014-85k-0304
Task No. NR627-846
TECHNICAL REPORT No. 7

DTIC FILE COPY

NMR, DSC, TMA, and High Pressure Electrical Conductivity Studies in PPO Complexed with Sodium Perchlorate

by

S.G. Greenbaum, Y.S. Pak, M.C. Wintersgill, J.J. Fontanella, J.W. Schultz, and C.G. Andeen

Hunter College of CUNY
Department of Physics
New York, NY 10021

July 1, 1987

DTIC
ELECTE
JUL 15 1987
S & D

Reproduction in whole or in part is permitted for any purpose of the United States Government.

This document has been approved for public release and sale; its distribution is unlimited.

87 7-14 067

REPORT DOCUMENTATION PAGE		READ INSTRUCTIONS BEFORE COMPLETING FORM
1. REPORT NUMBER 7	2. GOVT ACCESSION NO. ADA182262	3. RECIPIENT'S CATALOG NUMBER
4. TITLE (and Subtitle) NMR, DSC, DMA, and High Pressure Electrical Conductivity Studies in PPO Complexed with Sodium Perchlorate		5. TYPE OF REPORT & PERIOD COVERED Interim Technical Report
		6. PERFORMING ORG. REPORT NUMBER
7. AUTHOR(s) S.G. Greenbaum, Y.S. Pak, M.C. Wintersgill, J.J. Fontanella, J.W. Schultz, and C.G. Andeen		8. CONTRACT OR GRANT NUMBER(s) N00014-85K-0304
9. PERFORMING ORGANIZATION NAME AND ADDRESS Hunter College of CUNY/ Physics Department 695 Park Avenue New York, NY 10021		10. PROGRAM ELEMENT, PROJECT, TASK AREA & WORK UNIT NUMBERS NR627-846
11. CONTROLLING OFFICE NAME AND ADDRESS Office of Naval Research/ Code 1113 800 N. Quincy Street Arlington, VA 22217		12. REPORT DATE July 1987
		13. NUMBER OF PAGES
14. MONITORING AGENCY NAME & ADDRESS (if different from Controlling Office)		15. SECURITY CLASS. (of this report)
		15a. DECLASSIFICATION/DOWNGRADING SCHEDULE
16. DISTRIBUTION STATEMENT (of this Report) Approved for public release and sale. Distribution unlimited		
17. DISTRIBUTION STATEMENT (of the abstract entered in Block 20, if different from Report)		
18. SUPPLEMENTARY NOTES Prepared for publication in Journal of the Electrochemical Society		
19. KEY WORDS (Continue on reverse side if necessary and identify by block number) Ion-conducting polymer, NMR, DSC, DMA, high pressure conductivity, poly(propylene oxide).		
20. ABSTRACT (Continue on reverse side if necessary and identify by block number)		

cont'd.

Audio frequency electrical conductivity, DSC, DMA, and ^{23}Na NMR measurements have been carried out on Parel 58 elastomer complexed with sodium perchlorate. (As Parel 58 is primarily poly(propylene oxide), it will be referred to as PPO.) The DSC and DMA measurements yield similar values for T_g which are about 72°C higher than the "central" T_g for uncomplexed PPO. In addition, the DSC studies show that the sodium perchlorate is insoluble above about 140°C . The conductivity measurements have been carried out in vacuum over the temperature range 290-380K and at pressures up to 0.65 GPa from 315-370K. From a VTF analysis E_a is found to be about 0.09 eV and T_0 is found to be about 45°C below the "central" glass transition temperature which is the same behavior observed previously for PPO complexed with lithium salts and for the α -relaxation in uncomplexed material. In addition, it is found that the vacuum activation volumes for the electrical conductivity and the α -relaxation are approximately the same when compared relative to T_0 . The ^{23}Na NMR measurements reveal the presence of both bound and mobile sodium species, the relative concentrations of which change by about a factor of ten over the temperature range -90 to $+90^\circ\text{C}$. In addition the mobile ^{23}Na resonance becomes motionally narrowed above T_g . The NMR results combined with the conductivity data imply that ion motion is controlled by large scale segmental motions of the polymer chains.



Accession For	
NTIS CRA&I	<input checked="" type="checkbox"/>
DTIC TAB	<input type="checkbox"/>
Unannounced	<input type="checkbox"/>
Justification	
By	
Distribution/	
Availability Codes	
Date	Avail and/or Special
A-1	

NMR, DSC, DMA, AND HIGH PRESSURE ELECTRICAL CONDUCTIVITY STUDIES IN PPO
COMPLEXED WITH SODIUM PERCHLORATE*

S. G. Greenbaum and Y. S. Pak

Physics Department

Hunter College of CUNY

New York, NY 10021

M. C. Wintersgill, J. J. Fontanella, and J. W. Schultz

Physics Department

U. S. Naval Academy

Annapolis, MD 21402

C. G. Andeen

Physics Department

Case Western Reserve University

Cleveland, OH 44106

Differential Scanning Calorimetry (DSC)

ABSTRACT

Audio frequency electrical conductivity, DSC, DMA, and ²³Na NMR measurements have been carried out on Parel 58 elastomer complexed with sodium perchlorate. (As Parel 58 is primarily poly(propylene oxide), it will be referred to as PPO.) The DSC and DMA measurements yield similar values for T_g which are about 72°C higher than the "central" T_g for uncomplexed PPO. In addition, the DSC studies show that the sodium perchlorate is insoluble above about 140°C. The conductivity measurements have been carried out in vacuum over the temperature range 290-380K and at pressures up to 0.65 GPa from 315-370K. From a VTF analysis E_a is found to be about 0.09 eV and T_0 is found to be about 45°C below the "central" glass transition temperature which is the same behavior observed previously for PPO complexed with lithium salts and for the α relaxation in uncomplexed material. In addition, it is found that the vacuum activation volumes for the electrical conductivity and the α relaxation are approximately the same when compared relative to T_0 . The ²³Na NMR measurements reveal the presence of both bound and mobile sodium species, the relative concentrations of which change by about a factor of ten over the temperature range -90 to +90°C. In addition the mobile ²³Na resonance becomes motionally narrowed above T_g . The NMR results combined with the conductivity data imply that ion motion is controlled by large scale segmental motions of the polymer chains.

INTRODUCTION

In recent papers, results for the temperature and pressure variation of electrical conductivity in PPO complexed with lithium salts along with the temperature and pressure variation of the α relaxation have been presented.^{1,2} The most important result of that work is that it was shown that to within experimental uncertainty, the temperature and pressure variation of the electrical conductivity was found to be the same as the temperature and pressure variation of the electrical relaxation time for the α relaxation. This provides quantitative evidence that, for PPO, ionic conductivity is controlled by large-scale segmental motions (conformational rearrangements of the polymer chain backbone³) characteristic of the glass-rubber transition. "Such rearrangements occur by a mechanism of hindered rotation around main chain bonds and involve cooperative thermal motions of individual chain segments. The hindrance to these 'micro-Brownian' motions can be described in terms of viscous or frictional forces which result from interactions of the moving segment with neighboring molecules or with segments within the same chain."³ However, in the earlier paper,² it was emphasized that the conductivity results alone could not be used to elucidate the transport mechanism as the shift in carrier concentration with temperature was unknown. In the present paper both electrical conductivity and nuclear magnetic resonance (NMR) measurements are carried out on PPO complexed with sodium perchlorate. The combination of the results provides strong evidence that the large scale segmental motions control ion motion. Also, DSC and DMA studies are reported for the same material.

EXPERIMENTAL

The techniques for performing audio frequency complex impedance/electrical relaxation measurements over a wide range of temperatures and pressures are given elsewhere.¹ The key element in the measurements is a CGA-82 microprocessor-controlled bridge operating at seventeen frequencies from $10\text{--}10^5$ Hz. Once again, the material studied was Parel 58 (Hercules, Inc.) elastomer which is a sulfur-vulcanizable copolymer of propylene oxide and allyl glycidyl ether. As the material is approximately 95% propylene oxide, it is referred to as PPO. Samples were obtained by solution casting using methanol as the solvent. The materials were dried at about 110°C under vacuum continuously provided by an Alcatel 2008 pump. All procedures including loading of the samples into the various sample holders were carried out in a dry box with a relative humidity of less than 5%.

In the present work, gold electrodes were vacuum evaporated onto the surfaces of the material in either a three-terminal or two-terminal configuration. The samples were about 1 mm thick and the electrodes about 4 mm in diameter.

The differential scanning calorimetry (DSC) studies were carried out using a DuPont 910 DSC controlled by a DuPont 990 console which was interfaced with an Apple II+ microcomputer. The dynamic mechanical analysis studies (DMA) were carried out using a DuPont 982 DMA controlled by another modified DuPont 990 console.

The ^{23}Na NMR measurements were performed at 81 MHz utilizing standard pulse techniques. Good signal-to-noise ratios were obtainable by

averaging 500-1000 free induction decays (FID's). Linewidths and relative intensities of the two resolvable lineshape components were extracted from the FID's by selective saturation and subtraction as discussed later. Temperatures were controlled to within $\pm 2^{\circ}\text{C}$ by a nitrogen flow system.

RESULTS

Thermal Analysis

The DSC results for $\text{PPO}_8\text{NaClO}_4$ are shown in Fig. 1. Results for uncomplexed PPO are included for comparison. It is clear that the complexed material is highly amorphous in that it exhibits a strong glass transition with a "central" T_g of about 283K (The "onset" T_g is about 278K and the "end" is at about 288K.) Consequently, T_g is about 72°C higher than for the uncomplexed material for which the "central" glass transition temperature is about 211K.¹ Similar results were obtained via DMA studies as seen in Fig. 2. An increase in T_g with the addition of salt to PPO is a well known phenomenon.⁴

In addition, in the DSC studies for $\text{PPO}_8\text{NaClO}_4$, a strong endothermic event is observed at about 140°C . In order to obtain information concerning this feature, the material was annealed at various temperatures, quenched to -150°C as rapidly as possible in situ, and the DSC studies repeated. Typical results for the quenched material after anneal at temperatures above 140°C are shown in Fig. 1c. In all cases, a strong glass transition typical of uncomplexed PPO is observed. In addition, there is a broad feature centered at about -20°C and a high temperature exothermic event followed by an endotherm. It is to be emphasized that such behavior was not observed for quenched material annealed below 140°C ,

all data being similar to Fig. 1b. Consequently, it is concluded that at about 140°C the salt comes out of solution. Support for this interpretation can be found in the work of Teeters and Frech⁵ who observed a finely divided crystalline solid in PPO-NaSCN above 165°C and showed that the Raman spectrum was the same as microcrystalline NaSCN. Electrical conductivity studies would be of interest, however, for the materials discussed so far the temperature at which salt precipitation occurs is outside the range of the present equipment. However, the authors have recently shown that for PPO₈NaI and PPO₈KSCN salt precipitation DSC endotherms are observed at 100°C and 60°C respectively.⁶ In both cases, the electrical conductivity follows VTF or WLF behavior (see the discussion below) for temperatures somewhat below the salt precipitation temperature, then becomes significantly less than the expected value as temperature increases further. In addition, the ²³Na NMR studies in PPO₈NaI show a drop in the ratio of the mobile to bound sodium ions at about the temperature of conductivity anomaly. Finally, the DSC studies for PPO₈KSCN show behavior analogous to the results of the Raman studies of Teeters and Frech for PPO₈NaSCN.⁵ Specifically, DSC features similar to that observed for the pure salt are observed in the polymer after heating above the salt precipitation temperature.

NMR

The ²³Na NMR results for PPO₈NaClO₄ bear a striking similarity to those obtained for cross-linked poly(dimethylsiloxane-ethylene oxide) (PDMS-EO) complexes with NaCF₃COO.^{7,8} An important feature common to both systems is the presence of two lineshape components throughout the

temperature range of about -100 to $+100^{\circ}\text{C}$. In the PPO complex, the two ^{23}Na 's are characterized by vastly different spin-lattice relaxation times (T_1). The short- T_1 (~ 0.2 - 30 ms) component is slightly narrower than the long- T_1 (~ 1 s) component at low temperatures, and undergoes substantial motional narrowing above T_g . The long T_1 resonance, on the other hand, does not appear to have a pronounced temperature dependence until about 75°C , at which point broadening is observed. The short- T_1 narrow line is therefore attributed to mobile Na^+ ions while a bound Na configuration gives rise to the broad line.

The two to three order of magnitude difference in T_1 's facilitated the acquisition of the separate lineshape components by selective saturation and subtraction. Free induction decays for the broad and narrow lines at two temperatures are shown in Fig. 3. Comparison of Figs. 3a (5°C) and 3b (35°C) highlights the temperature insensitivity of the broad line, while comparison of Figs. 3a and 3c demonstrates the similarity (except for their T_1 values) between the broad and narrow lines just below T_g .

The ratio of the narrow line to broad line intensities (N/B) as a function of reciprocal temperature is plotted in Fig. 4. Perhaps the most crucial feature of the data in Fig. 4 is that the mobile ion concentration increases by only one order of magnitude over a temperature range in which the conductivity increases by five orders of magnitude. Therefore, carrier generation plays only a minor role in the conductivity mechanism. Comparison of Fig. 4 with conductivity data to be discussed later further highlights the relatively weak temperature dependence of the mobile Na^+ generation. The small decrease in N/B observed at the higher temperature

end of the plot is not presently understood. Another phenomenon which merits further study is the observation of a transition from first to second-order quadrupole broadening of the bound Na resonance above about 75°C. A similar observation was noted in the PDMS/EO complex, although the latter transition occurs at about 25°C, and was attributed to the dissociation of ion triplets (i.e. Na_2X^+ or NaX_2^-) into neutral ion pairs and single ions.⁵ However, this model conflicts with the above-mentioned high temperature decrease in N/B, unless the majority of the triplet species are NaX_2^- , whose dissociation would not yield additional Na^+ ions. Therefore, the possibility that the broad resonance may be attributable to Na bonded to the polymer chains must be explored.

As deduced from temperature and pressure-dependent conductivity and dielectric loss measurements to be discussed later, the primary mechanism believed to drive the ionic conductivity is large scale segmental motion associated with the glass-rubber transition. Figure 5 is a plot of the mobile Na resonance linewidth (obtained by saturating the bound resonance) as a function of temperature. It is clear from the data that the onset of motional narrowing occurs in the vicinity of the glass transition temperature, again indicating the importance of polymer chain motion to ionic mobility. The increase in linewidth above 60°C is due to rapid spin-lattice relaxation ($T_1 \leq 300 \mu\text{s}$) which introduces a lifetime broadening contribution to the total linewidth.

Electrical Conductivity

The techniques used to obtain values of the electric conductivity from complex impedance or admittance measurements are given elsewhere.^{1,2}

The results of a typical vacuum data run are shown in Fig. 6. The curvature often observed for amorphous polymer systems is apparent. Consequently, the conductivity data were first analyzed via the VTF equation:⁹

$$\sigma = AT^{-1/2} \exp^{-[E_a/k(T-T_0)]} \quad (1)$$

with the adjustable parameters A, E_a , and T_0 . A non-linear least squares fit of Eq. (3) to the data was carried out and the results are $E_a=0.096$ eV, $T_0=237.6$ K, and $\log_{10}A((\Omega\text{-cm})^{-1}\sqrt{K})=0.71$. The RMS deviation in $\log_{10}\sigma$ was 0.012.

The vacuum value for T_0 is about 45°C lower than the "central" $T_g=283$ K which was determined by DSC and DMA. Similar results have also been recently reported for PPO complexed with lithium salts^{1,2} and for poly(dimethyl siloxane-ethylene oxide) co-polymer containing a sodium salt.^{7,8} This result is consistent with the configurational entropy model^{10,11} where T_0 is interpreted as the temperature of zero configurational entropy which would be expected to occur at a much lower temperature than DSC or DMA T_g 's.

Next, isothermal data (data taken at a fixed temperature and various pressures) were taken and typical results are similar to those shown elsewhere for PPO complexed with lithium salts.^{1,2} A least squares fit of the following equation:

$$\log_{10}\sigma = \log_{10}\sigma_0 + aP + bP^2 \quad (2)$$

to the isothermal data was carried out and the resultant fitting parameters, $\log_{10}\sigma_0$, a , and b , are listed in Table I. The data were used to determine activation volumes directly via:

$$\Delta V^* = -kT \, d \ln \sigma / dP \quad (3)$$

The vacuum values are also listed in Table I. The activation volumes for $\text{PPO}_8\text{NaClO}_4$ and the previous results for PPO complexed with lithium salts¹ are plotted in Fig. 7 vs. $T-T_0$. The plot shows that the activation volume is approximately the same for all materials at a given temperature interval above T_0 . Consequently, different vacuum activation volumes can merely be attributed to different T_0 's.

In addition, the activation volume associated with the electrical relaxation time for the α relaxation was calculated from:

$$\Delta V^* = -kT \, d \ln \tau / dP \quad (4)$$

where τ is the electrical relaxation time. The results are also plotted in Fig. 7. It is seen that to within the scatter in the data, on the "reduced plot" they are the same as those obtained from the electrical conductivity. This provides strong, albeit indirect evidence that electrical conductivity is controlled by the same mechanism as the α relaxation. It has been known for many years that the α relaxation is due to large scale segmental motions of the polymer chains.³ Consequently, since the NMR results described above show that carrier generation plays only a minor role in electrical conductivity, the results show that ion

motion is controlled by large scale segmental motions of the polymer chains.

It is also noted that the activation volume calculated from Eq. (3) decreases as temperature increases. This agrees with previous observations in PEO^{12,13}. Further, this is expected since in general activation volumes scale with activation energy and, as is apparent from Fig. 6, the activation energy (slope of the conductivity plot) clearly decreases as temperature increases.

Next, the data were analyzed in terms of the WLF equation:¹⁴

$$\log_{10} \frac{\sigma(T)}{\sigma(T_g)} = \frac{C_1(T-T_g)}{C_2+(T-T_g)} \quad (5)$$

The resultant parameters for $T_g=283K$ are $C_1=10.5$, $C_2=44.7K$, and $\log_{10}((\sigma(T_g)(\Omega\text{-cm})^{-1}))=-11.2$. The RMS deviation was 0.01. The values of C_1 and C_2 are reasonably close to the "universal" values of 17.4 and 51.6K.¹⁵

Finally, for completeness, the data were analyzed via the mathematically equivalent VTF eq. in the form:

$$\sigma = A' \exp^{-[E'_a/k(T-T'_0)]} \quad (6)$$

The best-fit parameters are $E'_a=0.093$ eV, $T'_0=238.3K$, and $\log_{10}A'((\Omega\text{-cm})^{-1})=-0.66$.

In previous papers, the authors have presented isobaric data or an isobaric analysis of isothermal data. In particular, high pressure VTF parameters were reported.^{1,2} When that procedure was attempted for

$\text{PPO}_8\text{NaClO}_4$, somewhat unusual results were obtained. Specifically, the best fit parameters for 0, 0.1, 0.2, and 0.3 GPa were $E_a=0.096, 0.091, 0.10,$ and 0.12 eV, respectively, and $T_0=238, 254, 263,$ and 267K , respectively. The unusual feature, which is a decrease in E_a from 0.096 to 0.091 as pressure increases from "vacuum" to 0.1 GPa may possibly be attributable, in part, to the effect of high pressure on the solubility of the salt. Specifically, it was shown above from the DSC studies that the salt comes out of solution at high temperature. If pressure were to decrease the solubility at high temperatures, the high temperature, high pressure results would be strongly affected and thus anomalous high pressure VTF parameters would be expected. Further work concerning this point is necessary.

SUMMARY

In summary, then, the following results have been obtained:

- (a) ^{23}Na NMR-determined mobile to bound sodium ratios exhibit a factor of ten increase over a temperature range (-90 to $+90^\circ\text{C}$) in which the conductivity increases by five orders of magnitude. Thus carrier generation plays a relatively minor role in the transport mechanism. Motional narrowing of the mobile ^{23}Na resonance is observed, with the onset of the narrowing occurring at T_g .
- (b) It has been found that the electrical conductivity in $\text{PPO}_8\text{NaClO}_4$ exhibits the same pressure and temperature dependence as the relaxation time for the α relaxation in uncomplexed PPO.
- (c) The combination of the NMR and electrical conductivity data provides evidence that ion motion is controlled by the large scale segmental motions of the polymer chains characteristic of the glass-rubber transition.

ACKNOWLEDGMENTS

The authors would like to thank Hercules, Inc. for supplying the Parel 58 elastomer. Ms. M. Chia is acknowledged for assistance with the NMR measurements and data analysis. This work was supported in part by the Office of Naval Research, and the PSC-CUNY Research Award Program.

REFERENCES

1. J. J. Fontanella, M. C. Wintersgill, M. K. Smith, J. Semancik, and C. G. Andeen, J. Appl. Phys., 60, 2665 (1986).
2. J. J. Fontanella, M. C. Wintersgill, J. P. Calame, M. K. Smith, and C. G. Andeen, Solid State Ionics, 18&19, 253 (1986).
3. N. G. McCrum, B. E. Read, and G. Williams, Anelastic and Dielectric Effects in Polymeric Solids, (Wiley, New York, 1967).
4. J. Moacanin and E. F. Cuddihy, J. Polymer Science: Part C, 14, 313 (1966).
5. D. Teeters and R. Frech, Solid State Ionics, 18&19, 271 (1986).
6. M. C. Wintersgill, J. J. Fontanella, S. G. Greenbaum, and K. J. Adamic, Proceedings of the International Symposium on Polymer Electrolytes, St. Andrews, Scotland, 17-19 June 1987, to be published in the British Polymer Journal.
7. K. J. Adamic, S. G. Greenbaum, M. C. Wintersgill, and J. J. Fontanella, J. Appl. Phys., 60, 1342 (1986).
8. M. C. Wintersgill, J. J. Fontanella, M. K. Smith, S. G. Greenbaum, K. J. Adamic, and C. G. Andeen, Polymer, 28, 633 (1987).
9. H. Vogel, Physik Z., 22, 645 (1921); V.G. Tammann and W. Hesse, Z. Anorg. Allg. Chem., 156, 245 (1926); G.S. Fulcher, J. Am. Ceram. Soc., 8, 339 (1925).
10. J. H. Gibbs and E.A. DiMarzio, J. Chem. Phys. 28 (1958) 373.
11. G. Adam and J.H. Gibbs, J. Chem. Phys. 43 (1965) 139.
12. J. J. Fontanella, M. C. Wintersgill, J. P. Calame, F. P. Pursel, D. R. Figueroa, and C. G. Andeen, Solid State Ionics, 9&10, 1139 (1983).
13. A. V. Chadwick, J. H. Strange, and M. R. Worboys, Solid State Ionics

9&10, 1155 (1983).

14. M. L. Williams, R. F. Landel, and J. D. Ferry, J. Am. Chem. Soc., 77, 3701 (1955).

15. H. Schneider, M. Brekner, and H. Cantow, Polymer Bulletin, 14, 479 (1985).

Table 1. Best fit parameters in equation 4 and zero pressure activation volumes.

Maximum pressure (GPa)	T(K)	RMS Deviation	$\log_{10} \sigma_0$ $(\Omega\text{-cm})^{-1}$	$a(\text{GPa})^{-1}$	$b(\text{GPa})^{-2}$	ΔV^* (cm^3/mol)
0.10	314.6	0.037	-6.833	-14.1	-18.0	84.7
0.21	319.1	0.0054	-6.485	-12.1	-17.5	73.8
0.25	328.6	0.0091	-5.875	-10.4	-10.0	65.5
0.33	338.2	0.040	-5.368	-7.97	-10.2	51.6
0.30	343.0	0.0093	-5.152	-7.48	-6.34	49.1
0.42	348.3	0.011	-4.938	-6.31	-7.71	42.1
0.53	363.8	0.011	-4.412	-5.32	-3.90	37.0
0.56	368.0	0.041	-4.288	-5.36	-3.73	37.7

FIGURE CAPTIONS

Figure 1. DSC plot for (a) uncomplexed PPO (b) as-prepared $\text{PPO}_8\text{NaClO}_4$, and (c) $\text{PPO}_8\text{NaClO}_4$ after having been annealed above 140°C . The data were taken at 10 K/min. The data for (b) and (c) are for the same sample plotted on the same scale. However, the data for (a) has not been normalized for sample mass and thus only the temperatures associated with the event are meaningful, not its magnitude.

Figure 2. DMA plot for (a) uncomplexed PPO and (b) as-prepared $\text{PPO}_8\text{NaClO}_4$. The data were taken at 5 K/min.

Figure 3. ^{23}Na free induction decays in $\text{PPO}_8\text{NaClO}_4$: (a) long- T_1 component at 5°C and (b) 35°C and the short- T_1 component at (c) 5° and (d) 35°C .

Figure 4. Reciprocal temperature plot of narrow to broad line intensity ratios in $\text{PPO}_8\text{NaClO}_4$.

Figure 5. ^{23}Na linewidth of the mobile sodium obtained by saturating the bound sodium resonance. The onset of motional narrowing occurs at about $T = T_g$. The high temperature broadening is attributable to rapid spin-lattice relaxation.

Figure 6. Arrhenius plot of the electrical conductivity data. The squares represent the datum points and the solid line is the best fit VTF equation (equation 1).

Figure 7. Vacuum activation volumes vs. reduced temperature for (a) x-the electrical relaxation time for the α relaxation from reference 1, (b) the electrical conductivity for: diamonds- $\text{PPO}_8\text{LiCF}_3\text{SO}_3$, squares- $\text{PPO}_8\text{LiClO}_4$, Δ - PPO_8LiI , \star - PPO_8LiSCN from reference 1, and (c) pentagons- $\text{PPO}_8\text{NaClO}_4$.

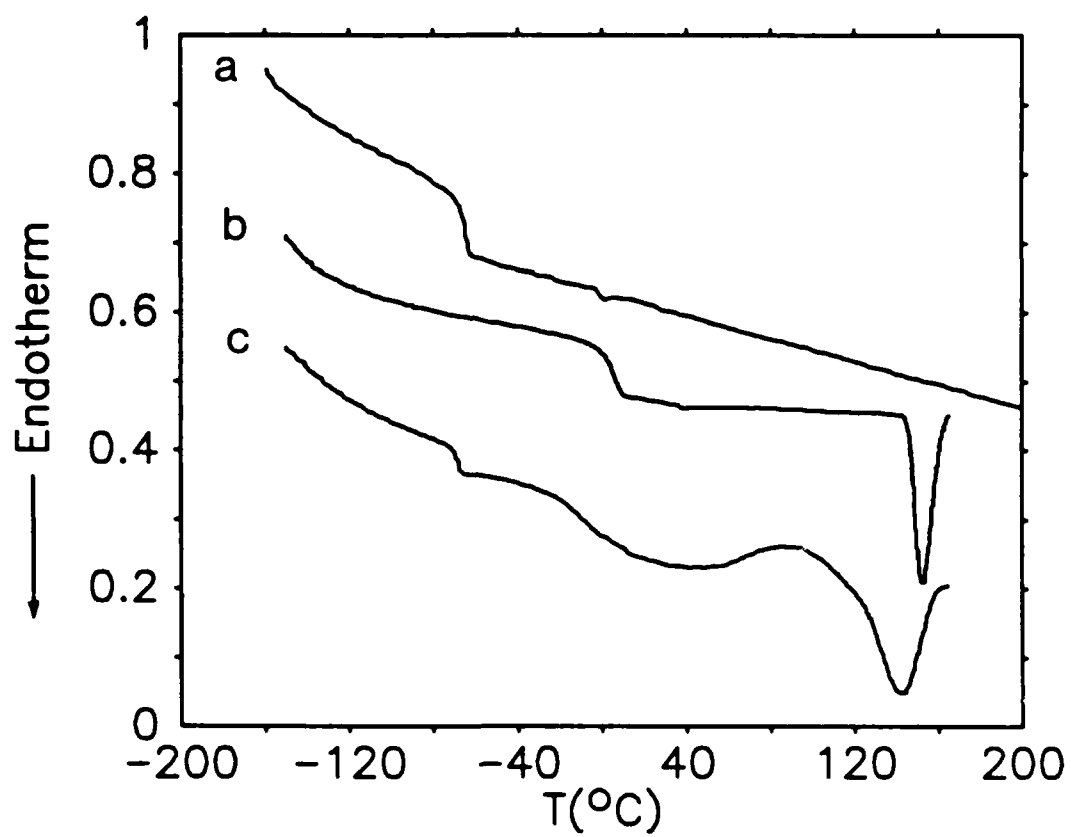


Figure 1

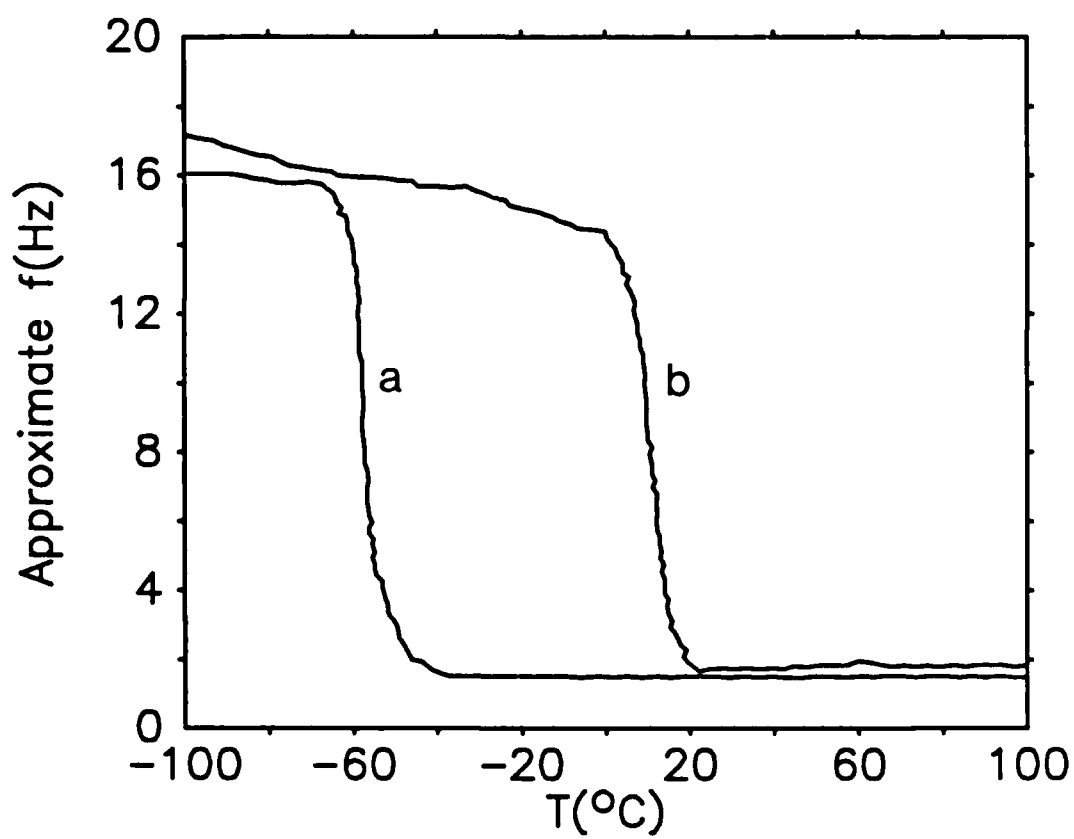


Figure 2

^{23}Na FID

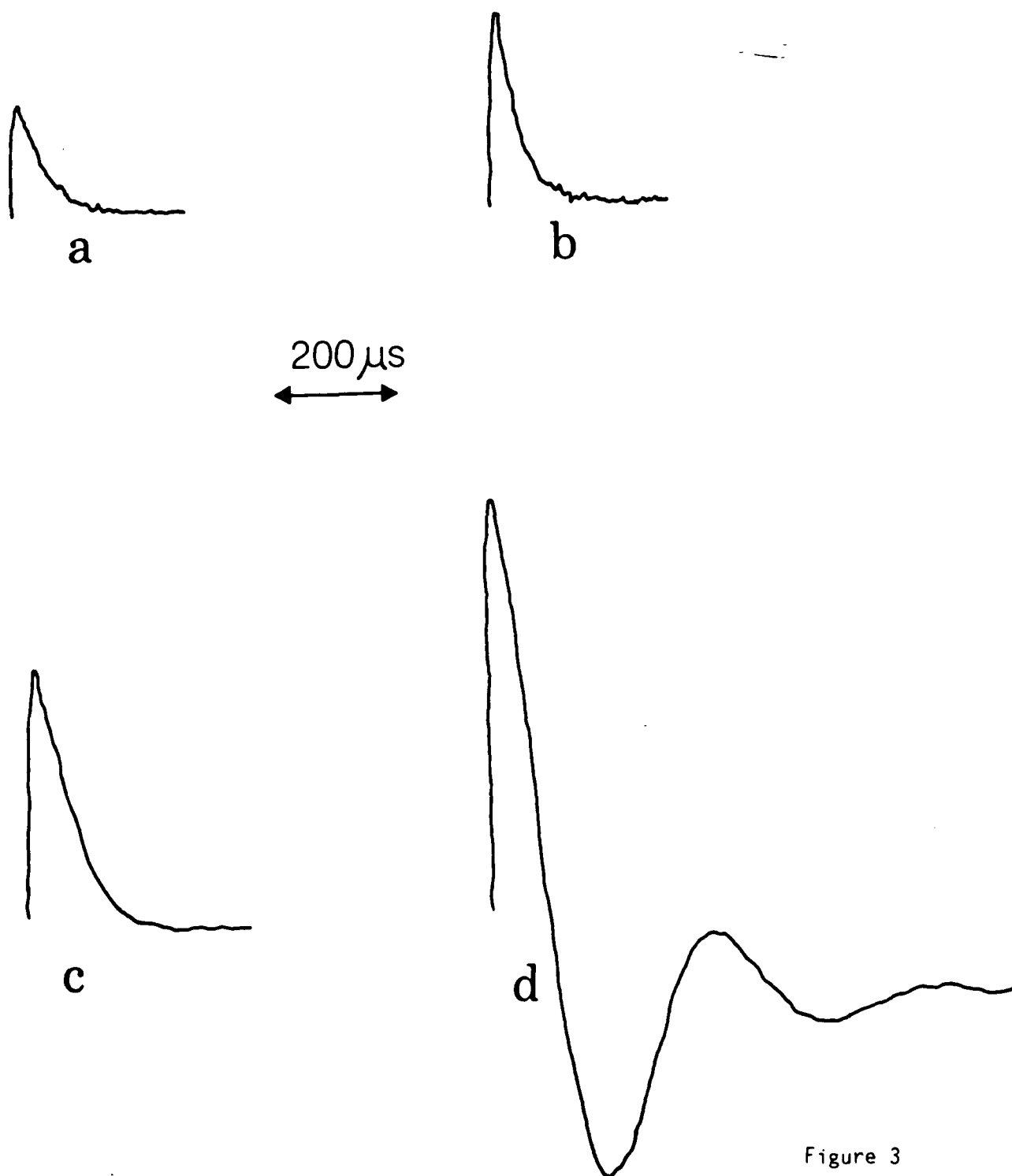
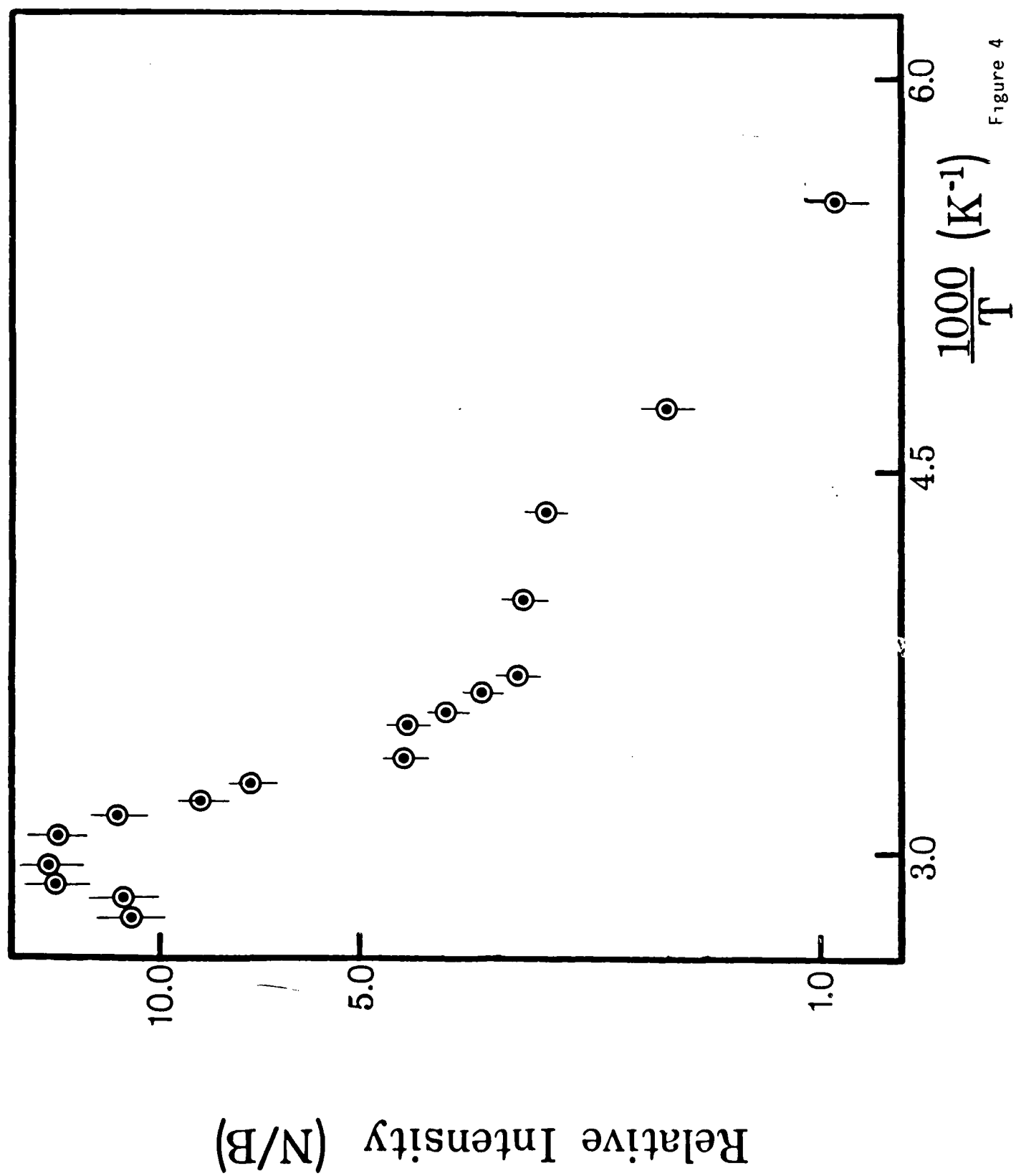


Figure 3



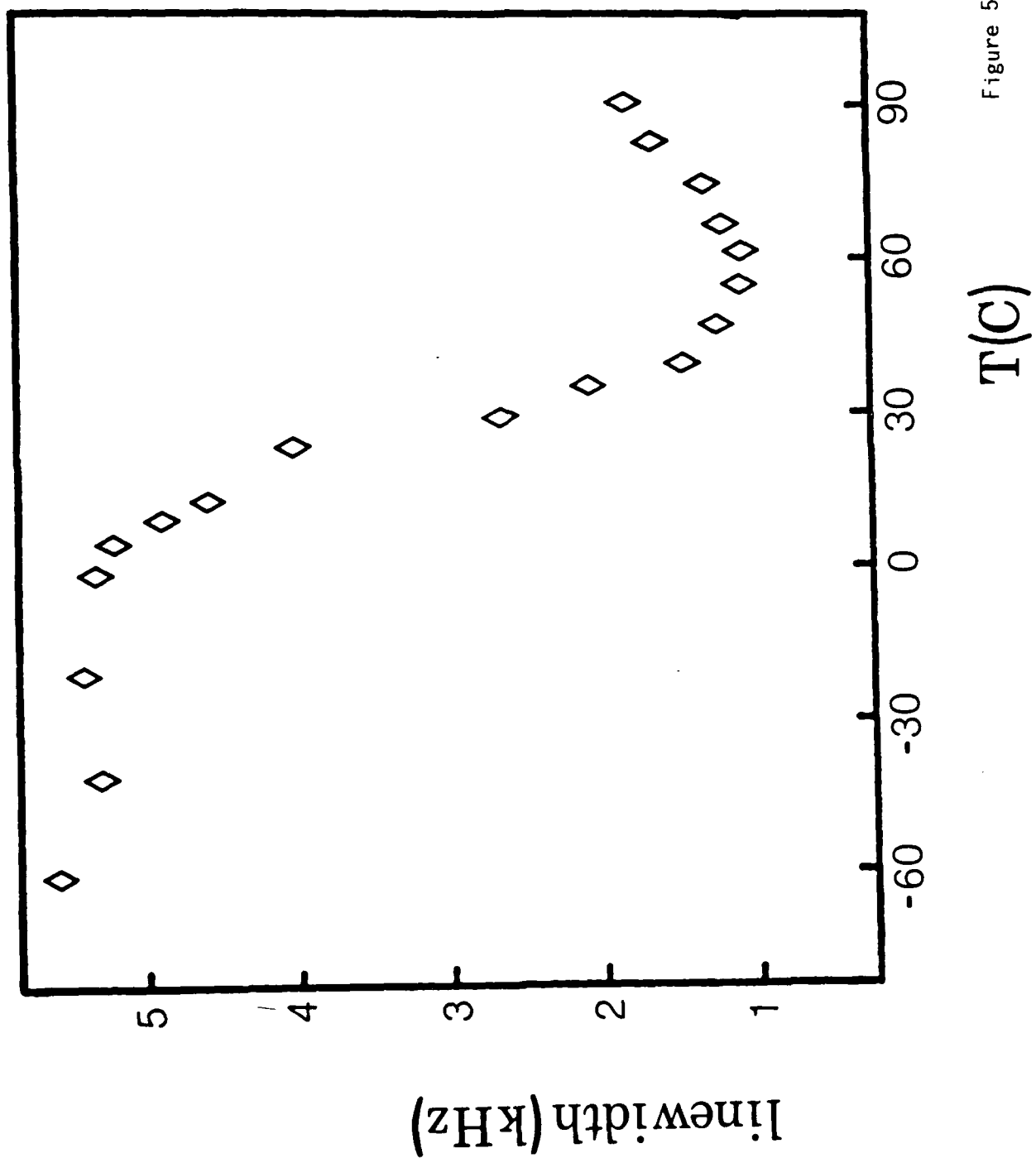


Figure 5

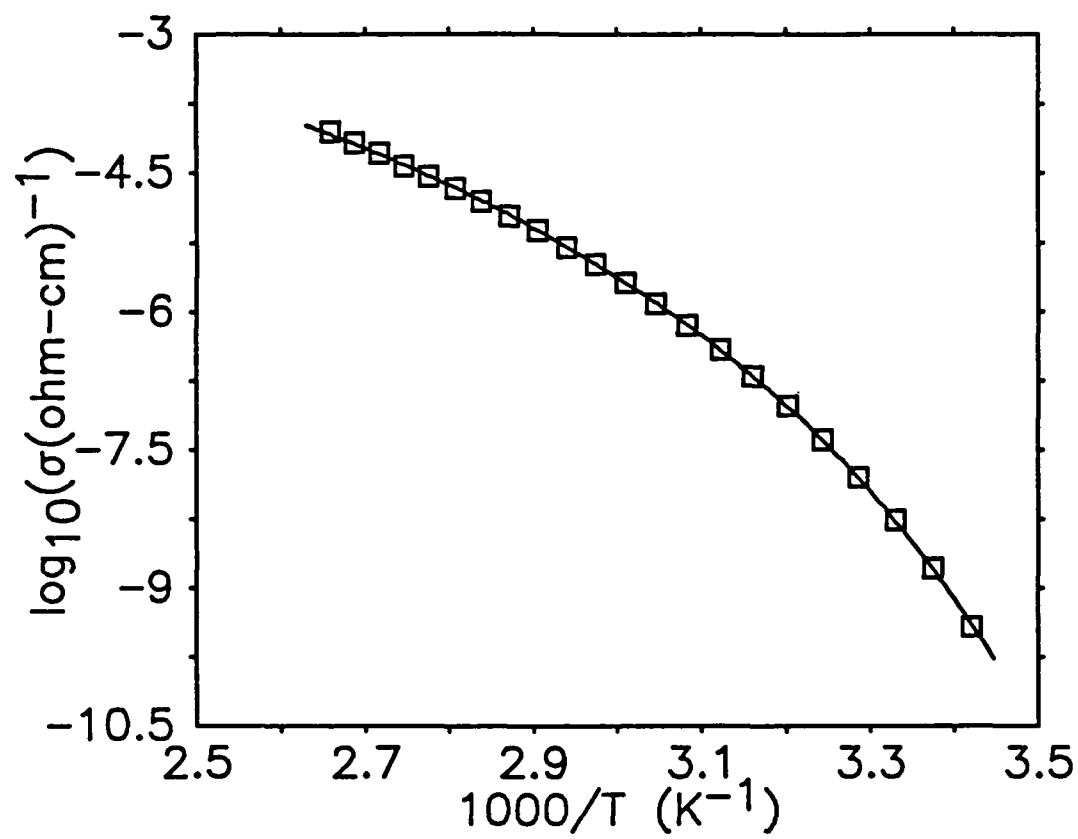


Figure 6

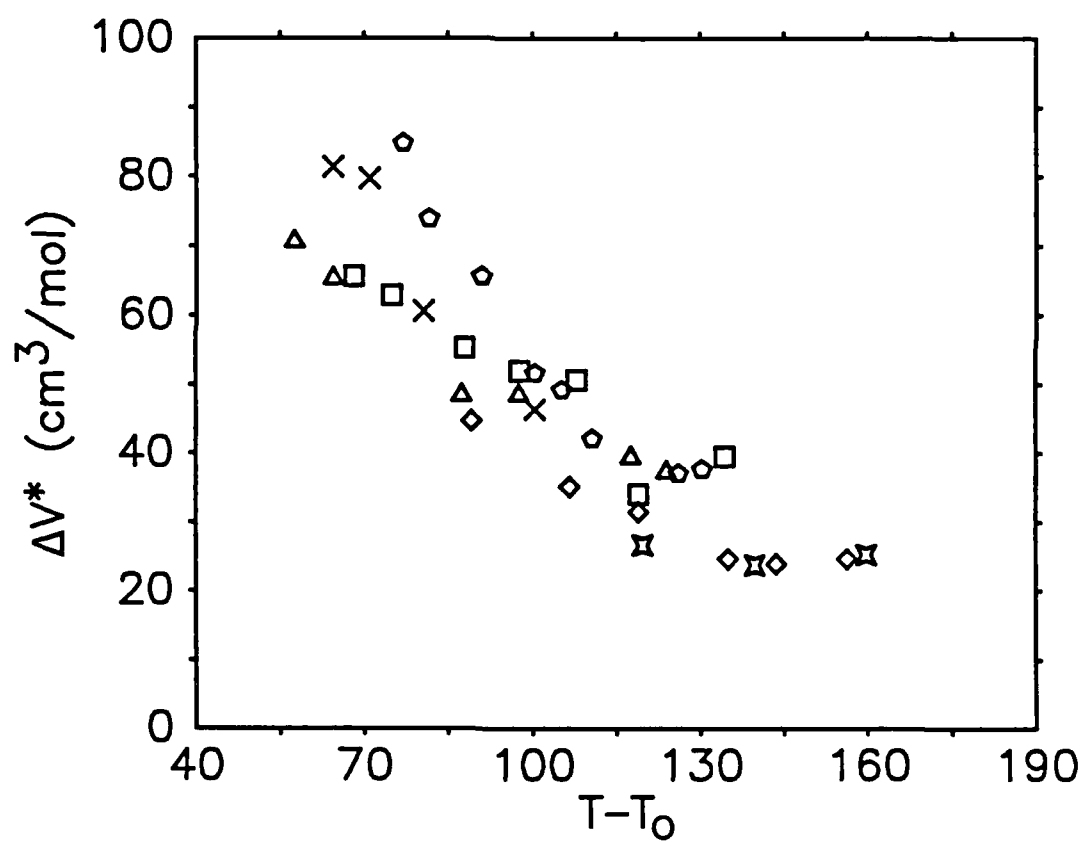


Figure 7

END

8-87

DTIC